Version 1.0 as of January 28, 2014

To be submitted to PRL

E06-014 INTERNAL DOCUMENT – NOT FOR PUBLIC DISTRIBUTION

A Precision Measurement of the Neutron Twist-3 Matrix Element d_2: Probing Color Forces

M. Posik,* D. Flay, W. Armstrong, A. Lukhanin, and Z.-E. Meziani†

Temple University, Philadelphia, PA 19122

D. S. Parno

Carnegie Mellon University, Pittsburgh, PA 15213 and
Center for Experimental Nuclear Physics and Astrophysics,
University of Washington, Seattle, WA 98195

K. Allada, C. Dutta, A. Kolarkar, and W. Korsch

University of Kentucky, Lexington, KY 40506

T. Averett, J. Katich, A. Kelleher, and B. Zhao

College of William and Mary, Williamsburg, VA 23187

F. Benmokhtar, G. B. Franklin, M. Friend, and V. Mamyan

Carnegie Mellon University, Pittsburgh, PA 15213

W. Bertozzi, W. Deconinck, S. Gilad, J. Huang, N. Muangma, and X. Zhan

Massachusetts Institute of Technology, Cambridge, MA 02139

A. Camsonne, J.-P. Chen, E. Chudakov, C.W. de Jager, A. Deur, J. Gomez, O. Hansen, D. W. Higinbotham, J.J. LeRose, R. Michaels, S. Nanda, A. Saha,‡ and B. Wojtsekhowski

Thomas Jefferson National Accelerator Facility, Newport News, VA 23606

M. Canan and S. Golge

Old Dominion University, Norfolk, VA 23529

G.D. Cates, M. M. Dalton, X. Deng, G. Jin, R. Lindgren, N. Liyanage, V. Nelyubin, B. Norum, S. Riordan, M. H. Shabestari, R. Subedi, A. Tobias, D. Wang, and X. Zheng

University of Virginia, Charlottesville, VA 22904

C. Chen, Z. Ye, and L. Yuan

Hampton University, Hampton, VA 23187

S. Choi

Seoul National University, Seoul, South Korea

F. Cusanno

INFN, Sezione di Roma, I-00161 Rome, Italy and
Istituto Superiore di Sanità, I-00161 Rome, Italy

L. El Fassi, G. Kumbartzki, and R. D. Ransome

Rutgers, The State University of New Jersey, Piscataway, NJ 08855

H. Gao

Duke University, Durham, NC 27708

F. Garibaldi

INFN, Sezione di Roma, I-00161 Rome, Italy

R. Gilman

Thomas Jefferson National Accelerator Facility, Newport News, VA 23606 and
Rutgers, The State University of New Jersey, Piscataway, NJ 08855

O. Glamazdin

Kharkov Institute of Physics and Technology, Kharkov 61108, Ukraine

L. Guo

Los Alamos National Laboratory, Los Alamos, NM 87545

T. Holmstrom and W. Troth

Longwood University, Farmville, VA 23909

C. Hyde

Old Dominion University, Norfolk, VA 23529 and
Université Blaise Pascal/IN2P3, F-63177 Aubière, France

H. F. Ibrahim

Cairo University, Giza 12613, Egypt

X. Jiang

Rutgers, The State University of New Jersey, Piscataway, NJ 08855 and
Los Alamos National Laboratory, Los Alamos, NM 87545

E. Long

Kent State University, Kent, OH 44242

D. McNulty

University of Massachusetts, Amherst, MA 01003

M. Mihovilovič

Jožef Stefan Institute, Ljubljana, Slovenia

B. Moffit and V. Sulkosky

Massachusetts Institute of Technology, Cambridge, MA 02139 and
Thomas Jefferson National Accelerator Facility, Newport News, VA 23606

A. Narayan and Nuruzzaman

Mississippi State University, MS 39762

Y. Oh

Kyungpook National University, Taegu 702-701, Republic of Korea

J. C. Peng and Y. Wang

University of Illinois at Urbana-Champaign, Urbana, IL 61801

X. Qian

Duke University, Durham, NC 27708 and

Kellogg Radiation Laboratory, California Institute of Technology, Pasadena, Ca 91125

Y. Qiang

Duke University, Durham, NC 27708 and
Thomas Jefferson National Accelerator Facility, Newport News, VA 23606

A. Rakhman

Syracuse University, Syracuse, NY 13244

B. Sawatzky

Temple University, Philadelphia, PA 19122 and
Thomas Jefferson National Accelerator Facility, Newport News, VA 23606

A. Shahinyan

Yerevan Physics Institute, Yerevan 375036, Armenia

S. Širca

University of Ljubljana, SI-1000 Ljubljana, Slovenia

P. Solvignon

Argonne National Lab, Argonne, IL 60439 and
Thomas Jefferson National Accelerator Facility, Newport News, VA 23606

X. Yan and Y. Ye

University of Science and Technology of China,
Hefei 230026, People's Republic of China

H. Yao

Temple University, Philadelphia, PA 19122 and
College of William and Mary, Williamsburg, VA 23187

Y. Zhang

Lanzhou University, Lanzhou 730000, Gansu, People's Republic of China

Y.-W. Zhang

Lanzhou University, Lanzhou 730000,
Gansu, People's Republic of China and
Rutgers, The State University of New Jersey, Piscataway, NJ 08855

(The Jefferson Hall A Collaboration)

(Dated: January 28, 2014)

Abstract

The double spin asymmetries and absolute cross-sections were measured at large Bjorken x, in both deep inelastic and resonance regions, by scattering longitudinally polarized electrons at beam energies of 4.74 and 5.89 GeV from a transversely and longitudinally polarized ^{3}He target. In this dedicated experiment, the spin structure function g_2 of ^{3}He was determined with precision at large x, and the neutron d_2^n twist-three matrix element was extracted. Combining d_2^n and the twist-four matrix element, f_2^n, the average color electric and magnetic forces were extracted and found to be of opposite sign and of about 60 MeV/fm

PACS numbers: 12.38.Aw, 12.38.Qk, 13.60.Hb, 13.88.+e, 14.20.Dh

* mposik1983@gmail.com

† meziani@temple.edu

‡ Deceased

Over the past 50 years, a wealth of information critical to our understanding of subatomic matter was obtained by probing the electromagnetic and spin structure of the nucleon through lepton (electron, muon an neutrino) scattering. More recently, the availability of polarized lepton beams and targets enabled an intensive worldwide experimental program of inclusive DIS measurements focused on the investigation of the nucleon spin structure function g_1. This led to the test of the Bjorken sum rule[1, 2], a fundamental sum rule of QCD, and the determination of the quarks spin contributions to the total nucleon spin[3]. Further investigation of the nucleon spin structure through QCD has shown that both spin structure functions (g_1 and g_2) of the nucleon contain contributions from the elusive quark-gluon correlations[4–6] beyond the perturbative-QCD radiative corrections [7–9]. However, in stark contrast with the case of g_1 where these correlations emerge at a higher order in the perturbative expansion, and thus are suppressed by powers of the inverse of Q^2 (the virtual photon probe four-momentum transfer squared), in that of g_2 they contribute at leading order. These correlations manifest themselves in $\bar{g}_2$, a deviation of the measured g_2 from the so-called Wandzura-Wilczek value g_2^{WW} [10] expressed solely in term of the g_1 spin structure function:

$$\bar{g}_2(x, Q^2) = g_2(x, Q^2) - g_2^{\mathrm{WW}}(x, Q^2); \tag{1}$$

$$g_2^{\mathrm{WW}}(x, Q^2) = -g_1(x, Q^2) + \int_x^1 g_1(y, Q^2)dy/y, \tag{2}$$

where x is the fraction of longitudinal momentum carried by the struck quark in the DIS process. At present there are no *ab initio* calculations of $\bar{g}_2$ yet. However, using the operator product expansion (OPE)[4, 6], the Q^2 dependent quantity

$$d_2 = 3\int_0^1 dx x^2 \bar{g}_2(x) = \int_0^1 dx x^2 \left[3g_2(x) + 2g_1(x)\right] \tag{3}$$

is shown to be related to a specific matrix element of *local* operators of quark and gluon fields[17, 19] and is calculable in lattice QCD [26]. Insight into the physical meaning of d_2 was articulated by Filippone and Ji [11] where d_2 is expressed in terms of a linear combination of χ_E and χ_B dubbed the electric and magnetic "color polarizabilities" respectively,

$$\chi_E \vec{S} = \frac{1}{2M^2}\langle P, S|q^\dagger \vec{\alpha} \times g\vec{E} q|P, S\rangle, \tag{4}$$

$$\chi_B \vec{S} = \frac{1}{2M^2}\langle P, S|q^\dagger g\vec{B} q|P, S\rangle, \tag{5}$$

where P and S are the nucleon momentum and spin, q and $q^\dagger$ are the quark fields, $\vec{E}$ and $\vec{B}$ the average color electric and magnetic fields seen by the struck quark, $\vec{\alpha}$ the velocity of the struck quark and g the strong coupling parameter.

More recently Burkardt [12] identified d_2 as proportional to the instantaneous average sum of the transverse electric $F_E^y(0)$ and magnetic $F_B^y(0)$ color forces the struck quark experiences at the instant it is hit by the virtual photon due to the remnant di-quark system in the DIS process. The net average force contributes in part to what is called the "color lensing" effect in semi-inclusive DIS where the struck quark feels color forces along its path out before turning into an outgoing hadron [12, 13]. The relations between color forces, color polarizabilities and the matrix elements of quark-gluon correlations are given by:

$$F_E^y(0) = -\frac{M^2}{4}\chi_E = -\frac{M^2}{4}\left[\frac{2}{3}\left(2d_2 + f_2\right)\right], \tag{6}$$

$$F_B^y(0) = -\frac{M^2}{2}\chi_B = -\frac{M^2}{2}\left[\frac{1}{3}\left(4d_2 - f_2\right)\right], \tag{7}$$

where f_2 is the other quark-gluon correlations matrix element, known as the twist-4 matrix element, and is related to the x^2 moment of the g_3 structure function. The twist-4 matrix element has never been directly measured but rather extracted by taking advantage of the Q^2 dependence of $g_1(x, Q^2)$[14, 15], since it appears as a higher order contribution suppressed by $1/Q^2$ in the first moment of g_1 namely $\Gamma_1 = \int_0^1 dx g_1(x, Q^2)$.

In fact, d_2 was calculated in different nucleon structure models [17, 18, 20–25] including lattice QCD calculations [26]. Consistently the different calculations give either zero or a small negative value deviating from the world measured *positive* value by about 2 standard deviations from zero [27, 28]. At the primordial level the forces represented in d_2 are in part responsible for the confinement of the constituents, measuring them and confirming our understanding of QCD is one of the important goals of hadronic physics. This situation called for a dedicated experiment in the case of the neutron.

The E06-014 experiment was performed at Jefferson Lab (JLab) in Hall A and ran from February to March of 2009. The experiment consisted of inclusive scattering of a longitudinally polarized electron beam off a transversely and longitudinally polarized ^{3}He target [30, 31] at two incident beam energies 4.74 GeV and 5.89 GeV. The scattered electrons with momenta ranging from 0.7 to 2 GeV/c were detected in both the BigBite spectrometer (BBS) and the left high resolution spectrometer (LHRS) [30, 31] set at a scattering angle of 45°. The double spin asymmetries (DSA) were measured over the full momentum range at once using the BBS due to its large momentum and angular acceptance while the unpolarized cross sections were obtained from the well understood LHRS by stepping over the same momentum range in discrete momentum steps. The longitudinal (transverse) DSA is defined as

$$A_{\parallel,(\perp)} = \frac{1}{P_t P_b D_{\mathrm{N}_2}(\langle\cos\phi\rangle)} \frac{N^{\downarrow\Uparrow(\Rightarrow)} - N^{\uparrow\Uparrow(\Rightarrow)}}{N^{\downarrow\Uparrow(\Rightarrow)} + N^{\uparrow\Uparrow(\Rightarrow)}}, \tag{8}$$

where N is the number of electrons, P_t is the target polarization, P_b is the electron polarization, D_{N_2} is the nitrogen dilution factor, ϕ is the azimuthal angle relative to the electron scattering plane, the single arrows refer to the electron's helicity direction, and the double arrows refer to the target's spin direction. The orientation of the arrows are such that arrows pointing to the right (left) represent spins that are transverse to the electron's momentum and arrows pointing up (down) represent spins being parallel (anti-parallel) to the electron's momentum.

The incident electron beam polarization was measured using two independent polarimeters based on Møller and Compton scattering, whose combined analysis yeilded an electron beam polarization of 71.87% $\pm$ 1.13% [32]. The residual beam charge asymmetry was determined to be smaller than 100 ppm through analysis of the Compton polarimeter data.

A 40 cm long polarized ^{3}He [30] cell was filled at room temperature with ~ 8 atm of ^{3}He and ~ 0.13 atm of N_2 (to reduce depolarization effects). The ^{3}He nuclei were polarized via a double spin-exchange optical pumping of a Rb-K mixture. The polarization was monitored by nuclear magnetic resonance (NMR) measurements approximately every 4 hours. The NMR measurements were calibrated with electron paramagnetic resonance (EPR) measurements and the longitudinal target polarization was cross-checked using known water NMR measurements. The average target polarization achieved was 50.49% $\pm$ 3.64%.

The BBS consists of a large-opening dipole magnet in front of the detector stack, which included three sets of multi-wire drift chambers for charged-particle tracking; a lead-glass calorimeter divided into pre-shower and shower sections, used for electron identification; a scintillator plane located between the pre-shower and shower layers, which provided additional electron identification; and a newly installed heavy gas Čerenkov detector [34] positioned between the second and third multi-wire drift chambers, which was used for pion rejection. The optics software package used for the BBS was calibrated using various targets at an incident energy of 1.2 GeV [34, 35]. The achieved angular and momentum resolutions were approximately 10 mrad and 1%, respectively. To keep trigger rates compatible with a high live time of the data acquisition ($\gtrsim 80\%$), the main electron trigger was formed from a geometrical overlap between the total shower energy (with a threshold set to ~ 500 MeV) and Čerenkov ADC sum (with threshold set to ~ 1.5 photoelectrons). Clean e^- identification was achieved by placing cuts on the pre-shower energy, the scintillator energy, the ratio E/p of the total shower energy to the momentum determined from optics reconstruction, and Čerenkov timing. These cuts resulted in a pion rejection factor that was better than 10^4:1.

The LHRS detector package consisted of two vertical drift chambers used for charged-particle tracking, two scintillator planes used for triggering and timing of charged particles, a light gas Čerenkov detector, and lead-glass calorimeter used for electron identification. Optics calibrations [35] for the HRS used the same targets that were used to calibrate the BigBite optics. The LHRS achieved a pion rejection factor better than 10^5:1, and measured the e^-–^{3}He inclusive cross section to better than 4%.

The two main sources of background contamination of the electron sample were due to produced charged pions and pair-produced electrons resulting from photons of π^0 decay. The BBS $\pi^\pm$ contamination was estimated from the analysis of the pre-shower energy spectrum and found to be less than 3% (6.5%) across the entire useful momentum acceptance for π^- (π^+). Weighting the measured $\pi^\pm$ asymmetries by the pion contamination resulted in a negligible $\pi^\pm$ asymmetry contamination. The $\pi^\pm$ contamination measured in the LHRS was also found to be negligible.

The amount of pair-produced electron contamination was estimated through positron measurements. Assuming symmetry between the pair produced electrons and positrons, the electron background was directly measured by reversing the BBS and LHRS magnet polarities resulting in positrons, rather than electrons, being steered into the detectors. By switching the magnet polarity both electrons and positrons see the same acceptance which drops out when forming the e^+/e^- ratio . The positron cross section was measured with the LHRS and subtracted from the electron cross section. We used the BBS measured and fitted e^+/e^- ratios, along with statistically weighted positron asymmetry measurements to determine the amount of pair production contamination in the electron sample. The final electron asymmetry was then computed from Eq. 9, where c_1 is the π^-/e^- ratio; c_2 is the π^+/e^+ ratio; c_3 is the e^+/e^- ratio; $A^m_{\perp,\parallel}$ is the measured electron asymmetry defined in Eqs. 8; and $A^{e^+}_{\perp,\parallel}$ is the measured positron asymmetry determined from Eqs. 8.

$$A^{e^-}_{\perp,\parallel} = \frac{A^m_{\perp,\parallel} - c_3 A^{e+}_{\perp,\parallel}}{1 - c_1 - c_3 + c_2 c_3}. \tag{9}$$

The electromagnetic internal and external radiative corrections were performed on the unpolarized cross section σ_0 using the formalism of Mo and Tsai [36, 37]. The elastic [36] and quasi-elastic [41] radiative tails were subtracted using form factors from [39] and [40]. The inelastic corrections were evaluated using the F1F209 model [48] for the unmeasured cross sections in the resonance and DIS regions. We followed the formalism of Akushevich *et al.* [43] to perform the radiative corrections on $\Delta\sigma_{\parallel}$ and $\Delta\sigma_{\perp}$, the polarized cross section differences. Here, the exact elastic polarized cross section difference tails were found to be negligible. The quasi-elastic [44, 45], resonance [46], and deep inelastic regions [50] were treated together using input from their respective models. The size of the total corrections in all cases did not exceed 45% of the measured σ_0, $\Delta\sigma_{\parallel}$, and $\Delta\sigma_{\perp}$. This resulted in an absolute uncertainty on the radiative corrections on g_1 and g_2, dominated by the input cross sections models dependence and the knowledge of thicknesses related to the target, of less than 5% at worst, thus smaller compared to their statistical uncertainty.

The DSA data were divided, in the Björken scaling variable x, into thirteen equally spaced bins of 0.05 bin width, while the cross sections were measured in about the same range but with different bin widths. The mean values of the x-bins ranged from $0.277 \leq x \leq 0.873$, covering a region from 0.25 to 0.90 in x. The corresponding Q^2 values ranged from 2.04 $\text{GeV}^2 \leq Q^2 \leq 4.88$ GeV^2 and 2.63 $\text{GeV}^2 \leq Q^2 \leq 6.59$ GeV^2 for incident beam energies of 4.74 GeV and 5.89 GeV, respectively. The Born cross sections were found to agree to within 6% with those of F1F209 cross section model [48] allowing us to obtain cross sections at the same x values as those used for the asymmetries through interpolations and extrapolations using the F1F209 model.

We show in Fig. 1 the polarized spin structure function g_2 on ^{3}He formed from the measured Born asymmetries and cross sections according to

$$g_2^{^3\text{He}} = \frac{MQ^2}{4\alpha^2}\frac{y^2\sigma_0}{(1-y)\,(2-y)} \times \left[-A_{\parallel}^{e^-} + \frac{1+(1-y)\cos\theta}{(1-y)\sin\theta}A_{\perp}^{e^-}\right] \tag{10}$$

where σ_0 is the ^{3}He Born cross section, α the electromagnetic coupling constant, $y = E - E'/E$ the fraction of the incident electron energy lost in the nucleon rest frame and θ the electron scattering angle. Note the dramatic improvement of the statistical precision of our data (in panel a)) compared to the existing world data at large $x \geq 0.3$. For clarity panel b) is zoomed in by a factor of 10 and with most of the world data removed.

The measured DSAs and cross sections at each beam energy were used to evaluate $d_2^{^3\mathrm{He}}$ at two mean $< Q^2 >$ values (3.21 and 4.32 GeV^2) according to

$$d_2^{^3\mathrm{He}} = \int_{0.25}^{0.90} dx \frac{MQ^2}{4\alpha^2} \frac{x^2 y^2 \sigma_0}{(1-y)(2-y)} \times \tag{11}$$
$$\left[\left(3 \frac{1+(1-y)\cos\theta}{(1-y)\sin\theta} + \frac{4}{y}\tan\frac{\theta}{2} \right) A_{\perp}^{e^-} + \left(\frac{4}{y} - 3 \right) A_{\parallel}^{e^-} \right].$$

The upper integration limit of $x = 0.90$ was chosen in order to avoid the quasielastic peak and the Δ resonance. In addition to using Eq. 12, the Nachtmann moments [55] were also used to evaluate $d_2^{^3\mathrm{He}}$. The difference between the two approaches at our kinematics was found to be an order of magnitude smaller than the measured $d_2^{^3\mathrm{He}}$ value, and so Nachtmann moments were not used in our analysis. The neutron information was extracted from the $d_2^{^3\mathrm{He}}$ quantity through the expression

$$d_2^n = \frac{d_2^{^3\mathrm{He}} - (2P_p - 0.014)\, d_2^p}{P_n + 0.056}, \tag{12}$$

where P_p and P_n are the effective proton and neutron polarizations in ^{3}He, and the factors 0.056 and 0.014 are due to the Δ-isobar contributions [33]. d_2^p in Eq. 12, was calculated from various global analyses [47, 50–54] using the x range covered by E06-014 at average $\langle Q^2 \rangle$ values of 3.23 and 4.32 GeV^2.

The d_2^n values measured during E06-014 represent only partial integrals. The full integrals can be evaluated by including the low and high x contributions. The low x contribution is suppressed due to the x^2 weighting of the d_2 integrand, but was calculated by fitting existing g_1^n [49, 56–58] and g_2^n [27, 56, 59] data. The fits to both structure functions extended the x range to $0.02 \leq x \leq 0.25$. The low x d_2^n contribution was assumed to have the same Q^2 value as our measured d_2^n values. To account for the high x contribution, the elastic form factors G_E^n and G_M^n were computed from the Galster parameterization [60] and dipole model, respectively. The contributions used to evaluate the total d_2^n integral are listed in Table I.

The total values of d_2^n results from this experiment are shown as a function of Q^2 in Fig. 2 (left panel) along with the world data. We find that our d_2^n results are in agreement with lattice QCD prediction [26], as well as various bag [17, 22, 23] and chiral soliton models [24, 25], which predict a zero or a small and negative value of d_2^n. Note the general agreement in the sign of our measured d_2^n compared to various model predictions. Given the precision of our measurements, although not at the same Q^2 value, we find a much smaller d_2^n value than that reported by the SLAC E155 experiment.

TABLE I. Our measured d_2^n, along with the low-x and elastic d_2^n contributions, which were used in evaluating the full d_2^n integrals.

$\langle Q^2 \rangle$ [GeV^2]	Measured	Low x	Elastic	Total
3.21	-0.00261	0.00038	-0.00108	-0.00331
4.32	0.00004	0.00038	-0.00069	-0.00027

TABLE II. Our results for f_2^n, F_E and F_B compared to model calculations. The value for d_2^n is assumed to be zero in the Instanton model calculation, as it is much smaller than f_2^n [64].

Group	Q^2 (GeV^2)	f_2^n	F_E (MeV/fm)	F_B (MeV/fm)
E06-014	3.21	0.07623 ± 0.00079 ± 0.04014	-51.85 ± 1.32 ± 29.90	66.64 ± 2.43 ± 30.00
E06-014	4.32	0.07329 ± 0.00083 ± 0.04013	-54.18 ± 1.37 ± 29.90	55.39 ± 2.53 ± 30.00
Instanton [64, 65]	0.40	0.038	-30.41	30.41
QCD sum rule [18, 19]	1	-0.013 ± 0.006	54.25 ± 15.52	79.52 ± 30.06
QCD sum rule [20]	1	0.010 ± 0.010	29.73 ± 16.62	81.75 ± 30.64
MIT Bag [17]	1	0.000	0.000	0.000

To extract the average electric and magnetic color forces, f_2^n needs to be determined first. To this end we followed the analysis of f_2 described in [14] but with updated a_2^n and d_2^n values as well as using data from JLab RSS experiment [62]. The singlet axial charge, $\Delta\Sigma$, was determined from values of Γ_1^n at $Q^2 > 5$ GeV^2 to be 0.375 ± 0.052, in excellent agreement with that found in [63]. A summary of our f_2^n and average color force values, along with comparisons to several models can be found in Table II.

In summary, we have measured the DSA and absolute cross sections from a polarized ^{3}He target. This allowed for the precision measurement of the neutron d_2 at two $\langle Q^2 \rangle$ values of 3.21 and 4.32 GeV^2. We find that d_2^n is in general small, and negative at lower $\langle Q^2 \rangle$, while consistent with zero at our higher $\langle Q^2 \rangle$ measurement. In contrast with previous results we find values consistent with the lattice QCD prediction [26], and various nucleon structure models. We used our d_2^n measurements to extract the twist-4 matrix element f_2^n and performed a neutron average electric and magnetic color forces decomposition. Our results show that f_2^n is much larger then d_2^n, leading to the electric and magnetic color forces to be nearly equal in magnitude but with opposite sign in the neutron.

We would like to thank the JLab Hall A technical staff and Accelerator Division for their outstanding support, as well as M. Burkardt, L. P. Gamberg, W. Melnitchouk, A. Metz, and J. Soffer for their useful discussions. This work was supported by DOE contract number DE-FG02-94ER40844 from Temple University and U.S. DOE Contract No. DE-AC05 84150, Modification No. M175, under which the Southeastern Universities Research Association, Inc. operates the Thomas Jefferson National Accelerator Facility.

---

[1] J. D. Bjorken, Phys. Rev. **148**, 1467 (1966).

[2] J. D. Bjorken, Phys. Rev. D **1**, 1376 (1970).

[3] C. A. Aidala, S. D. Bass, D. Hasch and G. K. Mallot, Rev. Mod. Phys. **85**, no. 2, 655 (2013) [arXiv:1209.2803 [hep-ph]].

[4] E. V. Shuryak and A. I. Vainshtein, Nucl. Phys. B **201**, 141 (1982).

[5] R. L. Jaffe, Comments Nucl. Part. Phys. **19**, 239 (1990).

[6] R. L. Jaffe and X. -D. Ji, Phys. Rev. D **43**, 724 (1991).

[7] V. N. Gribov and L. N. Lipatov, Sov. J. Nucl. Phys. **15**, 438 (1972) [Yad. Fiz. **15**, 781 (1972)].

[8] G. Altarelli and G. Parisi, Nucl. Phys. B **126**, 298 (1977).

[9] Yu. L. Dokshitzer, Sov. Phys. JETP **46**, 641(1977).

[10] S. Wandzura and F. Wilczek, Phys. Lett. B **72**, 195 (1977).

[11] B. W. Filippone and X. -D. Ji, Adv. Nucl. Phys. **26**, 1 (2001) [hep-ph/0101224].

[12] M. Burkardt, arXiv:0810.3589 [hep-ph].

[13] M. Burkardt, Nucl. Phys. A **735**, 185 (2004) [hep-ph/0302144].

[14] Z. -E. Meziani, W. Melnitchouk, J. -P. Chen, S. Choi, T. Averett, G. Cates, C. W. de Jager and A. Deur *et al.*, Phys. Lett. B **613**, 148 (2005) [hep-ph/0404066].

[15] M. Osipenko, W. Melnitchouk, S. Simula, P. E. Bosted, V. Burkert, M. E. Christy, K. Griffioen and C. Keppel *et al.*, Phys. Lett. B **609**, 259 (2005) [hep-ph/0404195].

[16] A. V. Sidorov and C. Weiss, Phys. Rev. D **73**, 074016 (2006) [hep-ph/0602142].

[17] X. -D. Ji and P. Unrau, Phys. Lett. B **333**, 228 (1994) [hep-ph/9308263].

[18] E. Stein, P. Gornicki, L. Mankiewicz, A. Schafer and W. Greiner, Phys. Lett. B **343**, 369 (1995) [hep-ph/9409212].

[19] E. Stein, P. Gornicki, L. Mankiewicz and A. Schafer, Phys. Lett. B **353**, 107 (1995) [hep-ph/9502323].

[20] I. I. Balitsky, V. M. Braun and A. V. Kolesnichenko, Phys. Lett. B **242**, 245 (1990) [Erratum-ibid. B **318**, 648 (1993)] [hep-ph/9310316].

[21] B. Ehrnsperger and A. Schafer, Phys. Rev. D **52**, 2709 (1995) [hep-ph/9505306].

[22] X. Song, Phys. Rev. D **54**, 1955 (1996) [hep-ph/9604264].

[23] M. Stratmann, Z. Phys. C **60**, 763 (1993).

[24] H. Weigel, L. P. Gamberg and H. Reinhardt, Phys. Rev. D **55**, 6910 (1997) [hep-ph/9609226].

[25] H. Weigel and L. P. Gamberg, Nucl. Phys. A **680**, 48 (2000) [hep-ph/0004057].

[26] M. Gockeler, R. Horsley, D. Pleiter, P. E. L. Rakow, A. Schafer, G. Schierholz, H. Stuben and J. M. Zanotti, Phys. Rev. D **72**, 054507 (2005) [hep-lat/0506017].

[27] P. L. Anthony *et al.* [E155 Collaboration], Phys. Lett. B **553**, 18 (2003) [hep-ex/0204028].

[28] X. Zheng *et al.* [Jefferson Lab Hall A Collaboration], Phys. Rev. C **70**, 065207 (2004) [nucl-ex/0405006].

[29] Jefferson Lab E07-003,
https://userweb.jlab.org/~rondon/sane/.

[30] J. Alcorn, B. D. Anderson, K. A. Aniol, J. R. M. Annand, L. Auerbach, J. Arrington, T. Averett and F. T. Baker *et al.*, Nucl. Instrum. Meth. A **522**, 294 (2004).

[31] Hall A Collaboration, JLab Hall A general operations manual,
http://hallaweb.jlab.org/news/minutes/OSP/osp-27feb2011.pdf (2011).

[32] D. Parno, Ph.D. thesis, Carnegie Mellon University,
http://hallaweb.jlab.org/experiment/E06-014/talks/DianaParno_Dissertation.pdf#Diana (2011).

[33] F. R. P. Bissey, V. A. Guzey, M. Strikman and A. W. Thomas, Phys. Rev. C **65**, 064317 (2002) [hep-ph/0109069].

[34] M. Posik, Ph.D. thesis, Temple University (2014).

[35] X. Qian *et al.* [Jefferson Lab Hall A Collaboration], Phys. Rev. Lett. **107**, 072003 (2011) [arXiv:1106.0363 [nucl-ex]].

[36] L. W. Mo and Y. -S. Tsai, Rev. Mod. Phys. **41**, 205 (1969).

[37] Y. -S. Tsai, SLAC-PUB-0848.

[38] K. Slifer *et al.* [E94010 Collaboration], Phys. Rev. Lett. **101**, 022303 (2008) [arXiv:0803.2267

[nucl-ex]].

[39] A. Amroun, V. Breton, J. M. Cavedon, B. Frois, D. Goutte, F. P. Juster, P. Leconte and J. Martino *et al.*, Nucl. Phys. A **579**, 596 (1994).

[40] J. W. Lightbody and J. S. O'Connell, Comp. in. Phys. **2(3)**, 57 (1988).

[41] S. Stein, W. B. Atwood, E. D. Bloom, R. L. Cottrell, H. C. DeStaebler, C. L. Jordan, H. Piel and C. Y. Prescott *et al.*, Phys. Rev. D **12**, 1884 (1975).

[42] I. V. Akushevich and N. M. Shumeiko, J. Phys. G **20**, 513 (1994).

[43] I. Akushevich, A. Ilyichev, N. Shumeiko, A. Soroko and A. Tolkachev, Comput. Phys. Commun. **104**, 201 (1997) [hep-ph/9706516].

[44] P. E. Bosted, Phys. Rev. C **51**, 409 (1995).

[45] J. E. Amaro, M. B. Barbaro, J. A. Caballero, T. W. Donnelly, A. Molinari and I. Sick, Phys. Rev. C **71**, 015501 (2005) [nucl-th/0409078].

[46] D. Drechsel, S. S. Kamalov and L. Tiator, Eur. Phys. J. A **34**, 69 (2007) [arXiv:0710.0306 [nucl-th]].

[47] D. de Florian, G. A. Navarro and R. Sassot, Phys. Rev. D **71**, 094018 (2005) [hep-ph/0504155].

[48] P. E. Bosted and V. Mamyan, arXiv:1203.2262 [nucl-th].

[49] P. L. Anthony *et al.* [E142 Collaboration], Phys. Rev. D **54**, 6620 (1996) [hep-ex/9610007].

[50] D. de Florian, R. Sassot, M. Stratmann and W. Vogelsang, Phys. Rev. Lett. **101**, 072001 (2008) [arXiv:0804.0422 [hep-ph]].

[51] C. Bourrely, J. Soffer and F. Buccella, Eur. Phys. J. C **23**, 487 (2002) [hep-ph/0109160].

[52] C. Bourrely, J. Soffer and F. Buccella, Phys. Lett. B **648**, 39 (2007) [hep-ph/0702221 [HEP-PH]].

[53] E. Leader, A. V. Sidorov and D. B. Stamenov, Phys. Rev. D **73**, 034023 (2006) [hep-ph/0512114].

[54] T. Gehrmann and W. J. Stirling, Phys. Rev. D **53**, 6100 (1996) [hep-ph/9512406].

[55] O. Nachtmann, Nucl. Phys. B **63**, 237 (1973).

[56] K. Kramer, D. S. Armstrong, T. D. Averett, W. Bertozzi, S. Binet, C. Butuceanu, A. Camsonne and G. D. Cates *et al.*, Phys. Rev. Lett. **95**, 142002 (2005) [nucl-ex/0506005].

[57] K. Abe *et al.* [E143 Collaboration], Phys. Rev. D **58**, 112003 (1998) [hep-ph/9802357].

[58] K. Abe *et al.* [E154 Collaboration], Phys. Lett. B **404**, 377 (1997) [hep-ex/9705017].

[59] P. L. Anthony *et al.* [E155 Collaboration], Phys. Lett. B **458**, 529 (1999) [hep-ex/9901006].

[60] S. Galster, H. Klein, J. Moritz, K. H. Schmidt, D. Wegener and J. Bleckwenn, Nucl. Phys. B **32**, 221 (1971).

[61] P. Solvignon *et al.* [E01-012 Collaboration], arXiv:1304.4497 [nucl-ex].

[62] K. Slifer *et al.* [Resonance Spin Structure Collaboration], Phys. Rev. Lett. **105**, 101601 (2010) [arXiv:0812.0031 [nucl-ex]].

[63] A. Accardi, J. L. Albacete, M. Anselmino, N. Armesto, E. C. Aschenauer, A. Bacchetta, D. Boer and W. Brooks *et al.*, arXiv:1212.1701 [nucl-ex].

[64] J. Balla, M. V. Polyakov and C. Weiss, Nucl. Phys. B **510**, 327 (1998) [hep-ph/9707515].

[65] N. -Y. Lee, K. Goeke and C. Weiss, Phys. Rev. D **65**, 054008 (2002) [hep-ph/0105173].

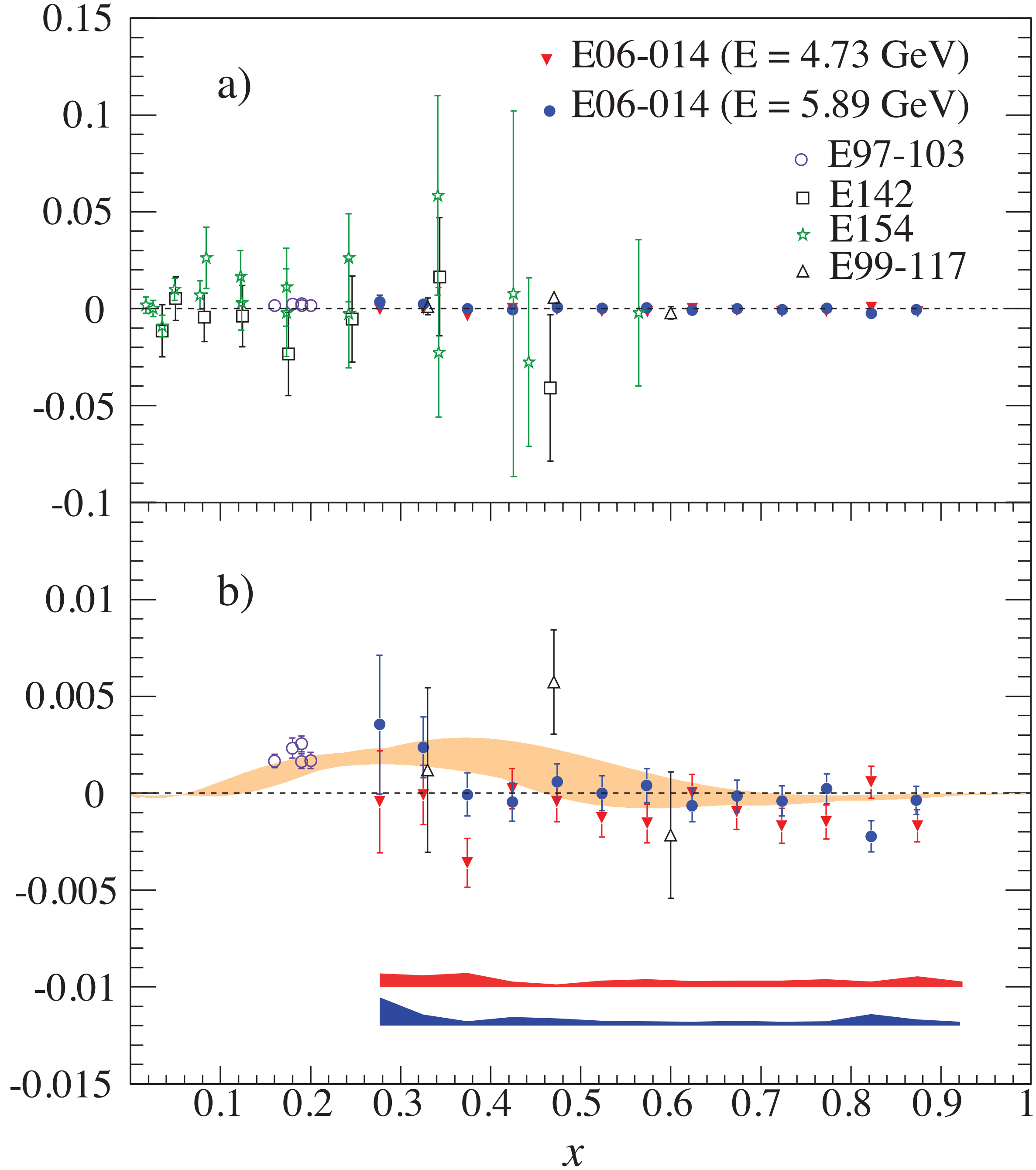

FIG. 1. x^2 weighted $g_2^{^3\mathrm{He}}$ plotted against x. Panel a) illustrates the increased precision of our results compared to the world data [28, 49, 56, 58]. All error bars in the world data are statistical and systematic uncertainties added in-quadrature. Panel b) is zoomed by a factor of 10 in the vertical scale and excludes some of the world data for clarity. The error bars on the E06-014 data are statistical only. The top (red) and bottom (blue) bands represent the systematic uncertainty associated with the E = 4.74 and 5.89 GeV data sets, respectively. The yellow band shows the $g_2^{\mathrm{WW},^3\mathrm{He}}$ coverage from several global analyses [47, 50–54].

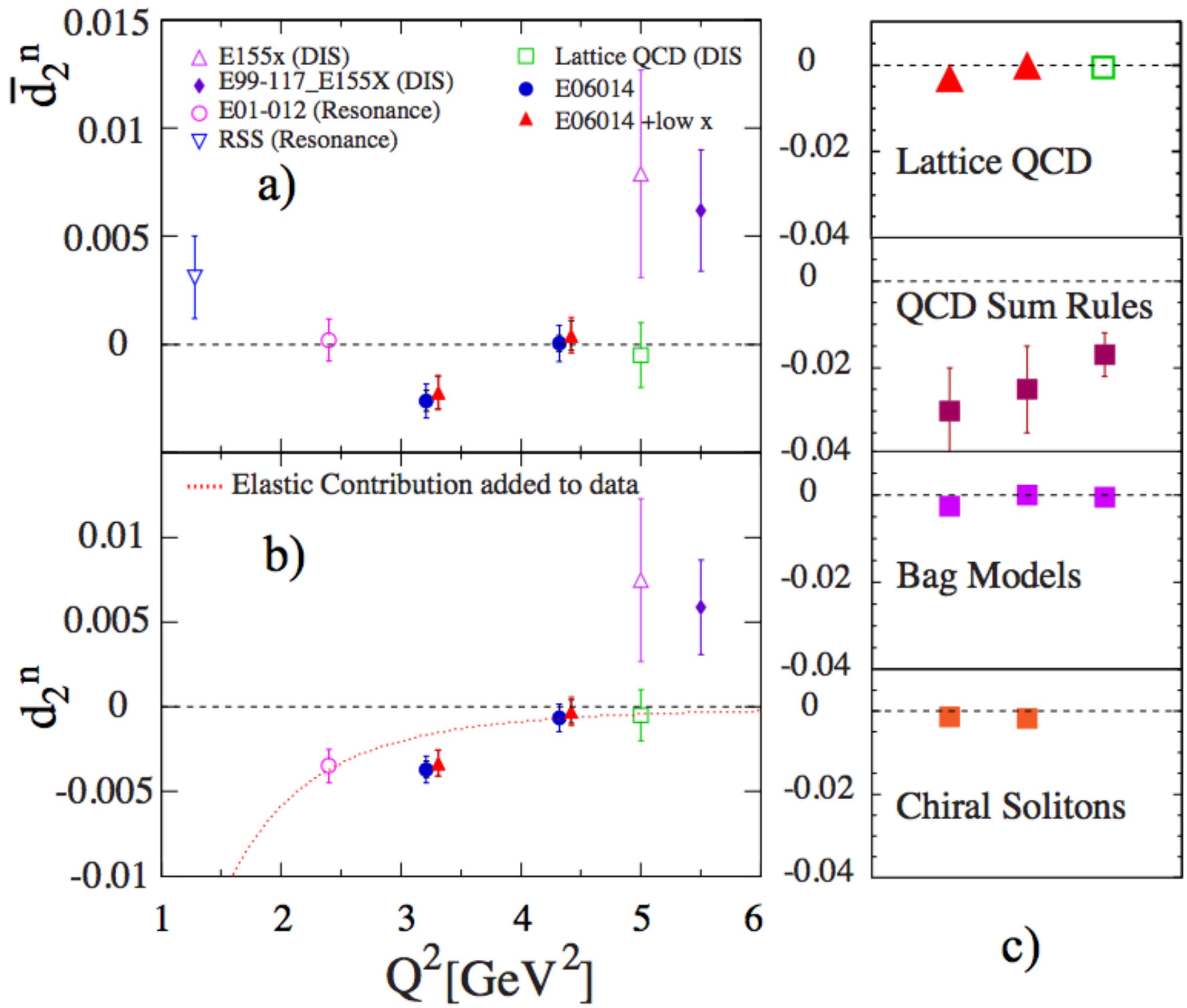

FIG. 2. Panel a): World $\bar{d}_2^n$ (no elastic contribution) data plotted against Q^2. The E06-014 measured d_2^n without (with) low the low x contributions added are represented by blue solid circle (solid red up triangle) markers, and are offset in Q^2 for clarity. The inner error bar ticks on the E06-014 measurements represent the systematic uncertainty, while the outer error bar ticks represent the statistical uncertainties. The world data [27, 28, 59, 61, 62] error bars represent the in-quadrature sum of the statistical and systematic uncertainties. Panel b): Shows the effect of adding the elastic contribution ($x = 1$ contribution already accounted for in the lattice QCD prediction). Panel c): d_2^n predictions from lattice QCD [26] (red up triangle markers are our final d2n values.), QCD sum rules [18, 20, 21], bag models [17, 22, 23], and chiral soliton models [24, 25].